nature geoscience

LETTERS

PUBLISHED ONLINE: 19 SEPTEMBER 2016 | DOI: 10.1038/NGEO2786

No evidence for Hadean continental crust within Earth's oldest evolved rock unit

J. R. Reimink[1,2*], J. H. F. L. Davies[3], T. Chacko[1], R. A. Stern[1], L. M. Heaman[1], C. Sarkar[1], U. Schaltegger[3], R. A. Creaser[1] and D. G. Pearson[1]

Due to the acute scarcity of very ancient rocks, the composition of Earth's embryonic crust during the Hadean eon (>4.0 billion years ago) is a critical unknown in our search to understand how the earliest continents evolved. Whether the Hadean Earth was dominated by mafic-composition crust, similar to today's oceanic crust[1–4], or included significant amounts of continental crust[5–8] remains an unsolved question that carries major implications for the earliest atmosphere, the origin of life, and the geochemical evolution of the crust–mantle system. Here we present new U–Pb and Hf isotope data on zircons from the only precisely dated Hadean rock unit on Earth—a 4,019.6 ± 1.8 Myr tonalitic gneiss unit in the Acasta Gneiss Complex, Canada. Combined zircon and whole-rock geochemical data from this ancient unit shows no indication of derivation from, or interaction with, older Hadean continental crust. Instead, the data provide the first direct evidence that the oldest known evolved crust on Earth was generated from an older ultramafic or mafic reservoir that probably surfaced the early Earth.

An understanding of the amount of continental crust produced in the first 500 million years of Earth history, and the resulting chemical differentiation of the Hadean silicate Earth, are critical parameters for developing robust geodynamical and geochemical models of our planet. Recently, evidence that the silicate Earth experienced very early (~4.4 billion years ago, Gyr) differentiation was discovered in the form of anomalous ^{142}Nd isotope signatures in ancient rocks[9–13]. These signatures, along with the recovery of zircon grains dated up to 4.4 Gyr (refs 4,5,7,8,14), imply that some type of crust existed on the young Earth, although the chemical nature of that crust, whether largely mafic, felsic, or some mixture, remains contentious[2–5,15,16]. To date, the rock and mineral record of Hadean crust dominantly consists of reputed 4.4–4.3 Gyr mafic rocks from northeastern Canada[10,17] and rare 4.0–4.4 Gyr detrital zircon grains recovered from quartzites and conglomerates in western Australia[4,5,7,8,14]. However, the composition of crystalline rocks parental to the Hadean detrital zircons remains controversial[4,5], as does the formation age of the mafic rocks from eastern Canada[18].

A variety of features preserved within Hadean detrital zircons motivated the uniformitarian view that the Hadean Earth contained nascent continental crust, possibly formed by tectonic processes similar to those that operate today[5,7,8]. An opposing view contends that Hadean crust was dominantly composed of mafic rocks formed and recycled in a geodynamic environment distinct from the modern Earth[1,2,4,10,16]. If significant Hadean continental crust did indeed exist, that crust would be expected to have compositions comparable to that which dominates the Archaean (2.5–4.0 Gyr) crustal rock record, namely the tonalite–trondhjemite–granodiorite (TTG) suite of granitoids, which are characterized by high La/Yb ratios[19]. However, coherent Hadean rock units are extraordinarily rare—hence the difficulty in evaluating the true extent and composition of Hadean crust.

We previously defined a new Hadean lithological unit—the Idiwhaa tonalitic gneiss—from the Acasta Gneiss Complex (AGC) of the Slave craton, Canada, which represents the oldest zircon-bearing Hadean rock suite known on Earth[20]. Here, we use published whole-rock elemental compositions, zircon trace-element and oxygen isotope data, in concert with new whole-rock geochemistry including Sm–Nd isotope analyses as well as high-precision U–Pb and split-stream U–Pb–Hf isotope analyses of well-characterized 4.02 Gyr zircons, to investigate the nature of Hadean crust.

Critical whole-rock geochemical features of the Idiwhaa unit include dominantly intermediate SiO_2 contents (~58–70 wt.% SiO_2), very high FeO contents, low magnesium numbers (Mg/[Mg+Fe]), and flat rare-earth-element (REE) patterns that are distinct from the steeper REE patterns of typical Archaean TTGs[19] (Supplementary Methods and Supplementary Figs 6–8). These geochemical features require high degrees of crystal fractionation of a water-poor basaltic magma at relatively shallow crustal levels[21]. Notably, the major-element characteristics of the Idiwhaa unit preclude derivation by partial melting of typical basaltic source rocks. Low to moderate degrees of melting (<40%) of such rocks yields sodic melts with lower FeO contents and generally higher silica contents than the Idiwhaa unit[19,22].

The Idiwhaa unit whole-rock REE patterns are in equilibrium with the REE patterns measured in >4.0 Gyr igneous zircon extracted from the unit, indicating that whole-rock compositions can reliably be used to infer the petrogenetic history of this unit and the zircons were formed by primary igneous crystallization from their current host rock[20]. Furthermore, whole-rock Sm–Nd isotope systematics of Idiwhaa unit samples (Supplementary Figs 11–13) are consistent with the zircon U–Pb crystallization age as well as the initial zircon Hf isotope data. A regression of the Sm–Nd isotope data obtained from these samples yields an imprecise date of 3,824 ± 270 Myr ($n = 9$). Although of low precision, the Sm–Nd date for Idiwhaa unit samples is significantly different from previously reported Sm–Nd ages of 3,370 Myr (Supplementary Fig. 13) produced by combining data from a wide variety of AGC rock units, but within uncertainty of the zircon U–Pb crystallization age. Initial εNd values calculated for individual Idiwhaa unit samples at 4,020 Myr range from −0.3 to −3.7, whereas the initial εNd of the 3,824 Myr regression line is −2.9. Although variable, these initial εNd values suggest that the Idiwhaa magma was derived from or

[1]Department of Earth and Atmospheric Sciences, University of Alberta, Edmonton, Alberta T6G 2E3, Canada. [2]Department of Terrestrial Magnetism, Carnegie Institution of Washington, Washington DC 20015, USA. [3]Department of Earth Sciences, University of Geneva, 1205 Geneva, Switzerland.
*e-mail: jreimink@carnegiescience.edu

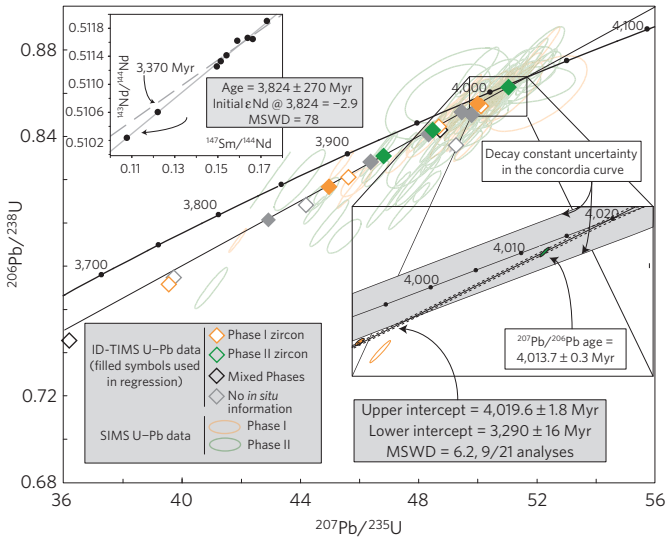

Figure 1 | Concordia plot of high-precision U–Pb data from the TC3 zircons. Large, light-coloured ellipses are previously reported SIMS U–Pb plotted at the 1σ level for clarity[20]. Symbols for the TIMS data are much larger than typical 2σ uncertainty and correspond to zircon growth phases (Methods). The upper intercept of a regression line through analyses containing the least recent Pb loss documents the crystallization age of the unit. Top-left inset shows whole-rock Sm–Nd isotope systematics of Idiwhaa unit samples with a variety of SiO_2 contents. The regression is within error of the crystallization age of the unit determined by zircon U–Pb. Bottom-right inset shows one-zircon analysis plots completely within the uncertainty band of concordia.

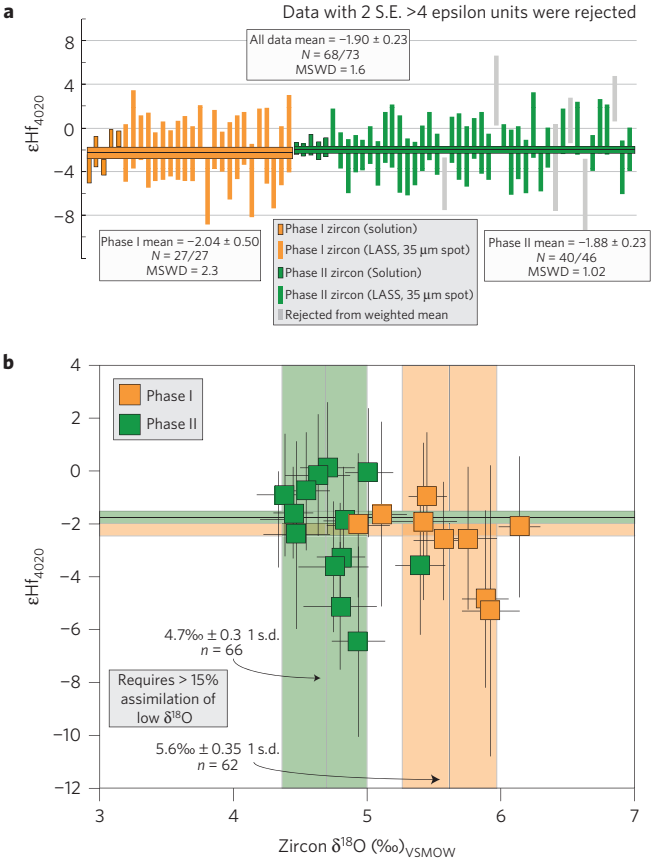

Figure 2 | Hafnium isotope analysis from 4,020 Myr zircon grains from Idiwhaa tonalitic gneiss sample TC3. a, Initial εHf values for two igneous phases of TC3 zircon, corrected to 4,020 Myr along with fully propagated uncertainties (Methods). There is no discernible initial Hf isotopic difference between Phase I and Phase II zircon material, suggesting the assimilant material was not significantly older evolved crust. **b**, Correlated Hf- and O-isotope data from TC3 zircon material plotted by growth phase. Also shown are the weighted means and 1 s.d. for both εHf and $\delta^{18}O$ of both phases. The 0.9‰ shift in $\delta^{18}O$ suggests ~35% assimilation of low $\delta^{18}O$ crust between magmatic zircon growth stages (Methods).

interacted with an enriched source, consistent with the zircon Hf isotope data discussed below.

The petrogenetic history of the Idiwhaa unit involved partial melting of the Hadean mantle to generate a primary basaltic magma that subsequently underwent extensive crystal fractionation. This iron-enriched magma then crystallized two phases (I and II) of igneous zircon. Phase I zircon comprises unzoned cores that are mantled by oscillatory-zoned Phase II zircon. Secondary ion mass spectrometric (SIMS) data indicate that both phases of zircon crystallized at ~4.02 Gyr (ref. 20). Using a novel technique for analysing complex zircons (Methods), we determined a highly precise age of 4,019.6 ± 1.8 Myr for the two phases of zircon growth (Fig. 1). Phase I zircon records $\delta^{18}O$ values (5.6 ± 0.35‰; $n = 62$) indistinguishable from mantle zircon (5.3 ± 0.3‰; ref. 23), whereas Phase II zircon has distinctly lower values (4.7 ± 0.30‰; $n = 66$; Fig. 2b)[20]. This ~0.9% drop in $\delta^{18}O$ values in two zircon phases yielding essentially identical ages suggests that, in the short time interval between Phase I and II zircon crystallization, the Idiwhaa magma assimilated crust that had previously been altered at high temperatures by surface waters[20].

The Hf-isotope composition of igneous zircon in the 4.02 Gyr Idiwhaa unit allows us to evaluate the Hadean mantle and pre-existing crust that was assimilated at the time of magma intrusion. The weighted mean of initial εHf values from Phase I zircon is −2.04 ± 0.50 (2 standard error, s.e.), a value indistinguishable from that of Phase II zircon (−1.88 ± 0.23, 2 s.e; Fig. 2a; Supplementary Information —Methods), despite their distinct oxygen isotope compositions (Fig. 2b). These Hf isotope data are in broad agreement with previous data from other, younger AGC zircons (3.5–3.9 Gyr) that reveal unradiogenic Hf isotopic compositions[24–26]. However, given our detailed understanding of the petrogenesis of the Idiwhaa unit, its Hf isotopic compositions provide a more robust determination of Hadean crustal compositions than was previously possible.

The Hf isotope data presented here indicate that the crustal assimilation process that occurred between Phase I and II zircon crystallization (documented in the zircon $\delta^{18}O$ values) could not have involved assimilation of very ancient (for example, ≥4.2 Gyr) continental crust of TTG-like composition, which is characterized by low Lu/Hf, and hence would have evolved to low εHf values by 4.02 Gyr. In such a scenario, assimilation causing the drop in $\delta^{18}O$ values observed in Phase II zircon growth would have also significantly decreased the εHf value of Phase II relative to Phase I zircon and generated much more fractionated whole-rock REE patterns (that is, high La/Yb) than those observed in the Idiwhaa unit (Fig. 3a). Moreover, small differences between the slopes of REE patterns in Phase I and Phase II zircons[20] are opposite to that expected if the late-stage assimilant had a TTG-like composition (Supplementary Figs 9 and 10), and potentially more in line with assimilation of mafic crust. It must be noted that assimilation of mafic crust at this late stage, even very old (4.4 Gyr) mafic crust, would not drastically change the Hf isotopic composition of Phase II zircon due to the generally low Hf contents of such crust.

The subchondritic εHf value of −2.04 ± 0.50 recorded by Phase I zircon (with mantle-like oxygen isotope compositions) is surprising and requires the involvement of an enriched (low Lu/Hf) source, as pristine mantle-derived magma would be expected to have chondritic or suprachondritic εHf values ≥0. To account for its major- and trace-element characteristics, the Idiwhaa unit must have been derived from or interacted with largely mafic or

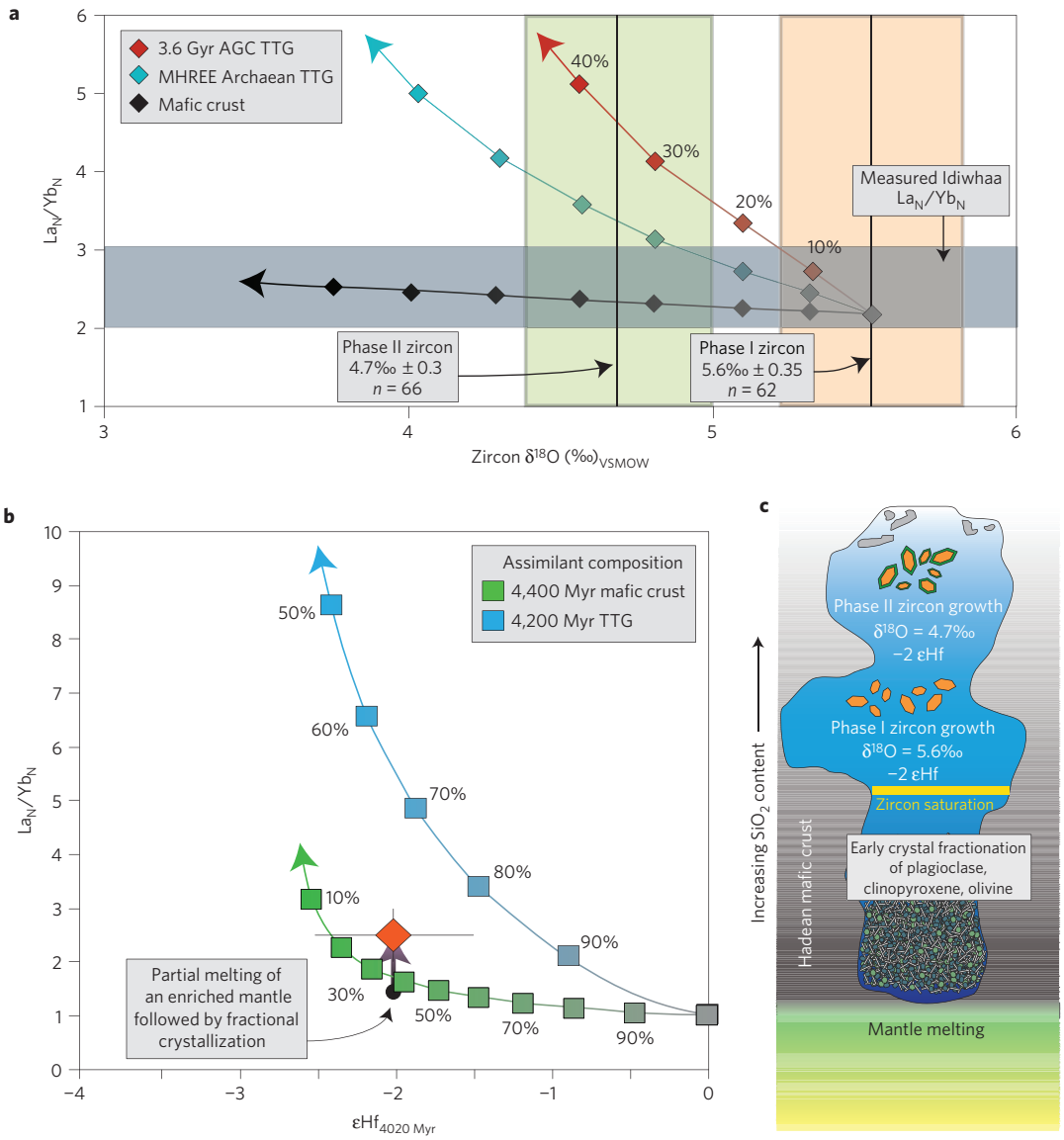

Figure 3 | Modelling results show lack of evidence for Hadean TTG-like crust during formation of the Idiwhaa unit. a–c, Results from modelling both the assimilation that occurred between zircon Phase I and Phase II growth (**a**) and AFC processes before zircon saturation (**b**), and a model for the petrogenesis of the Idiwhaa unit (**c**). In both cases, assimilation of TTG-like crust cannot explain the chemical signatures within the Idiwhaa unit. However, either assimilation of very ancient mafic crust or partial melting of an enriched mantle followed by significant fractional crystallization, and eventual late-stage assimilation of hydrated basaltic crust, can explain all aspects of the Idiwhaa unit. The Idiwhaa field is defined by the mean and 1 s.d. of intermediate SiO_2 Idiwhaa samples. Percentages in **b** are the % liquid remaining, as opposed to percentage mixing in **a**.

ultramafic source rocks. However, the negative initial εHf and εNd values of the unit indicate that the source rocks or assimilants must have also had long-term enrichments in incompatible trace elements (that is, long-term low Lu/Hf and Sm/Nd).

One possible explanation for the observed negative εHf and εNd values is assimilation by the Idiwhaa magma of pre-existing TTG-composition continental crust before Phase I zircon crystallization. Indeed, the reported occurrence of one 4.2 Gyr xenocrystic zircon core from the AGC[27] indicates the presence of evolved crust even older than the Idiwhaa unit. However, a −2 unit shift in εHf values of a chondritic-composition primary magma cannot be generated by assimilation of 4.2 Gyr TTG-like crust without also significantly increasing the La_N/Yb_N (where N denotes chondrite-normalized concentration) of the Idiwhaa unit (Fig. 3b). It is possible that assimilation of a small amount of still older (~4.4 Gyr) TTG crust at an early stage of magma evolution, when magma Hf contents were still low, would be able to generate a 2 unit decrease in εHf values without shifting the La_N/Yb_N of the Idiwhaa unit outside of measured compositions. However, we consider this scenario highly unlikely for two reasons. First, we have already ruled out TTG assimilation at the later, documented assimilation event that occurred in the Idiwhaa magma between Phase I and II zircon growth (Fig. 3a). Therefore, if assimilation of very ancient TTG crust did occur, it would have to occur only at an early stage of magma evolution, while not occurring later, to change the εHf value without significantly disturbing the REE systematics of the Idiwhaa unit. Second, no evidence for >4.2 Gyr zircon-bearing silicic crust exists within the AGC despite thousands of zircons analysed. If significant amounts of very old felsic crust were indeed present at depth in the AGC, more reports of ancient xenocrystic zircon would be expected from the complex. Other mechanisms for generating the negative εHf and εNd values of the Idiwhaa unit appear to be required.

All aspects of the major- and trace-element compositions of the Idiwhaa unit before zircon crystallization can be explained by

closed-system fractional crystallization of a primary mantle-derived basalt magma. In that case, the −2 εHf value of the parental magma would have to be inherited from an enriched mantle source that was characterized by long-term low Lu/Hf (Fig. 3b) (Methods). Another way to generate the combination of geochemical features observed in the Idiwhaa unit is for a primary mantle-derived basaltic magma with chondritic Hf-isotope compositions to assimilate an early-formed, enriched mafic crust, similar in elemental and isotopic composition to lunar KREEP, which had by 4.02 Gyr evolved to negative εHf values[2,28]. In this scenario, a large degree of assimilation of this mafic crust could occur without appreciably changing the La_N/Yb_N of the Idiwhaa magma (Fig. 3b).

Although the ultimate source of the negative initial εHf value remains somewhat enigmatic, our combined whole-rock and zircon Hf- and O-isotope data set suggest that the Hadean-age Idiwhaa unit was both generated from and intruded into a mafic to ultramafic environment, without significant involvement of Hadean continental crust. This inference of a mafic-dominated Hadean crust is consistent with some recent estimates of Hadean crustal composition derived from the composition of melts parental to the Jack Hills zircon suite[2,4], the mafic composition of presumed 4.3–4.4 Gyr rocks from Nuvvuagittuq[10,17], and a lack of evidence for significant Hadean continental crust in other ancient gneiss terranes[2,3,16]. Collectively, geochemical data may support a vision that the Hadean Earth was surfaced by long-lived mafic/ultramafic crust with variably enriched compositions. In such a setting, evolved, zircon-bearing rock suites are formed by fractionation of a primitive basaltic magma at shallow levels, followed by assimilation/partial melting of much older mafic crust[1,2,29]. The longevity of isotopically enriched Hadean crustal or mantle domains such as those documented here and in Greenland[11], along with their depleted counterparts[9,30], implies that processes operating on the earliest Earth were distinctly different from the modern paradigm of plate tectonics, and may suggest a unique Hadean geodynamic setting[30].

Methods

Methods, including statements of data availability and any associated accession codes and references, are available in the online version of this paper.

Received 19 October 2015; accepted 13 July 2016; published online 19 September 2016

References

1. Kamber, B. S., Collerson, K. D., Moorbath, S. & Whitehouse, M. J. Inheritance of early Archaean Pb-isotope variability from long-lived Hadean protocrust. *Contrib. Mineral Petrol.* **145,** 25–46 (2003).
2. Kemp, A. I. S. *et al*. Hadean crustal evolution revisited: new constraints from Pb–Hf isotope systematics of the Jack Hills zircons. *Earth Planet. Sci. Lett.* **296,** 45–56 (2010).
3. Kemp, A. I. S., Hickman, A. H., Kirkland, C. L. & Vervoort, J. D. Hf isotopes in detrital and inherited zircons of the Pilbara craton provide no evidence for Hadean continents. *Precambr. Res.* **261,** 112–126 (2015).
4. Nebel, O., Rapp, R. P. & Yaxley, G. M. The role of detrital zircons in Hadean crustal research. *Lithos* **190–191,** 313–327 (2013).
5. Harrison, T. M. The Hadean crust: evidence from >4 Ga zircons. *Annu. Rev. Earth Planet. Sci.* **37,** 479–505 (2009).
6. Harrison, T. M. Heterogeneous Hadean hafnium: evidence of continental crust at 4.4 to 4.5 Ga. *Science* **310,** 1947–1950 (2005).
7. Wilde, S. A., Valley, J. W., Peck, W. H. & Graham, C. M. Evidence from detrital zircons for the existence of continental crust and oceans on the Earth 4.4 Gyr ago. *Nature* **409,** 175–178 (2001).
8. Mojzsis, S. J., Harrison, T. M. & Pidgeon, R. T. Oxygen-isotope evidence from ancient zircons for liquid water at the Earth's surface 4,300 Myr ago. *Nature* **409,** 178–181 (2001).
9. Caro, G., Bourdon, B., Birck, J. L. & Moorbath, S. ^{146}Sm–^{142}Nd evidence from Isua metamorphosed sediments for early differentiation of the Earth's mantle. *Nature* **423,** 428–432 (2003).
10. O'Neil, J., Carlson, R. W., Francis, D. & Stevenson, R. K. Neodymium-142 evidence for Hadean mafic crust. *Science* **321,** 1828–1831 (2008).
11. Rizo, H. *et al*. The elusive Hadean enriched reservoir revealed by ^{142}Nd deficits in Isua Archaean rocks. *Nature* **491,** 96–99 (2012).
12. Rizo, H., Boyet, M., Blichert-Toft, J. & Rosing, M. Combined Nd and Hf isotope evidence for deep-seated source of Isua lavas. *Earth Planet. Sci. Lett.* **491,** 96–99 (2011).
13. Roth, A. S. G. *et al*. Combined $^{147,146}Sm$-$^{143,142}Nd$ constraints on the longevity and residence time of early terrestrial crust. *Geochem. Geophys. Geosyst.* **15,** 2329–2345 (2014).
14. Froude, D. O. *et al*. Ion microprobe identification of 4,100–4,200 Myr-old terrestrial zircons. *Nature* **304,** 616–618 (1983).
15. Bowring, S. A. & Housh, T. The Earth's early evolution. *Science* **269,** 1535–1540 (1995).
16. Kamber, B. S., Whitehouse, M. J., Bolhar, R. & Moorbath, S. Volcanic resurfacing and the early terrestrial crust: zircon U–Pb and REE constraints from the Isua Greenstone Belt, southern West Greenland. *Earth Planet. Sci. Lett.* **240,** 276–290 (2005).
17. O'Neil, J., Carlson, R. W., Paquette, J.-L. & Francis, D. Formation age and metamorphic history of the Nuvvuagittuq Greenstone Belt. *Precambr. Res.* **220–221,** 23–44 (2012).
18. Roth, A. S. G. *et al*. Inherited ^{142}Nd anomalies in Eoarchean protoliths. *Earth Planet. Sci. Lett.* **361,** 50–57 (2013).
19. Moyen, J.-F. & Martin, H. Forty years of TTG research. *Lithos* **148,** 312–336 (2012).
20. Reimink, J. R., Chacko, T., Stern, R. A. & Heaman, L. M. Earth's earliest evolved crust generated in an Iceland-like setting. *Nature Geosci.* **7,** 529–533 (2014).
21. Grove, T. L. & Kinzler, R. J. Petrogenesis of andesites. *Annu. Rev. Earth Planet. Sci.* **14,** 417–454 (1986).
22. Rapp, R. P. *et al*. Partial melting of amphibolite/eclogite and the origin of Archean trondhjemites and tonalites. *Precambr. Res.* **51,** 1–25 (1991).
23. Valley, J. W., Kinny, P. D., Schulze, D. J. & Spicuzza, M. J. Zircon megacrysts from kimberlite: oxygen isotope variability among mantle melts. *Contrib. Mineral Petrol.* **133,** 1–11 (1998).
24. Amelin, Y., Lee, D. C., Halliday, A. N. & Pidgeon, R. T. Nature of the Earth's earliest crust from hafnium isotopes in single detrital zircons. *Nature* **399,** 252–255 (1999).
25. Iizuka, T. *et al*. Reworking of Hadean crust in the Acasta gneisses, northwestern Canada: evidence from *in-situ* Lu–Hf isotope analysis of zircon. *Chem. Geol.* **259,** 230–239 (2009).
26. Guitreau, M. *et al*. Lu–Hf isotope systematics of the Hadean–Eoarchean Acasta Gneiss Complex (Northwest Territories, Canada). *Geochim. Cosmochim. Acta* **135,** 251–269 (2014).
27. Iizuka, T. *et al*. 4.2 Ga zircon xenocryst in an Acasta gneiss from northwestern Canada: evidence for early continental crust. *Geology* **34,** 245–248 (2006).
28. Taylor, D. J., McKeegan, K. D. & Harrison, T. M. Lu–Hf zircon evidence for rapid lunar differentiation. *Earth Planet. Sci. Lett.* **279,** 157–164 (2009).
29. Kamber, B. S. The evolving nature of terrestrial crust from the Hadean, through the Archaean, into the Proterozoic. *Precambr. Res.* **258,** 48–82 (2015).
30. Debaille, V., O'Neill, C., Brandon, A. D. & Haenecour, P. Stagnant-lid tectonics in early Earth revealed by ^{142}Nd variations in late Archean rocks. *Earth Planet. Sci. Lett.* **373,** 83–92 (2013).

Acknowledgements

J. Ketchum and the Northwest Territories Geological Survey staff are thanked for scientific and field support, without which this project would not have been possible; E. Thiessen and R. Reimink are thanked for mapping and field assistance. F.X. D'Abzac is thanked for assistance with solution Hf isotope analyses at the University of Geneva and Y. Luo is thanked for assistance with LA-ICPMS split stream Hf-U-Pb analyses. A. Oh and K. Nichols are thanked for laboratory support during ion probe analyses. A review from J. O'Neil vastly improved this work. This research was funded by National Science and Engineering Research Council of Canada Discovery Grants to T.C. and L.M.H., as well as Canada Excellence Research Chairs Program funding to D.G.P., support from the University of Geneva and the Swiss National Science Foundation to J.H.F.L.D. and U.S., and a Circumpolar/Boreal Alberta Research grant for fieldwork to J.R.R.

Author contributions

J.R.R., T.C. and J.H.F.L.D. conducted mapping and sample collection. J.R.R. carried out sample crushing, processing and zircon separations. J.H.F.L.D. and J.R.R. carried out collection of bulk zircon Hf and U–Th–Pb isotopic data. C.S., J.R.R. and D.G.P. collected zircon laser-ablation Hf and U–Pb data. R.A.C. collected whole-rock Nd isotope data. Modelling was conducted by J.R.R. and T.C. All authors contributed to discussion of the results and their implications, as well as preparation of the manuscript.

Additional information

Supplementary information is available in the online version of the paper. Reprints and permissions information is available online at www.nature.com/reprints. Correspondence and requests for materials should be addressed to J.R.R.

Competing financial interests

The authors declare no competing financial interests.

Methods

Sample descriptions. All samples reported here were identified in the field and later geochemically confirmed as parts of the same 4.02 Gyr rock unit, a unit we have previously identified and informally termed the Idiwhaa tonalitic gneiss[20]. These samples share the following key field characteristics; they are relatively melanocratic, containing significant biotite and amphibole, as well as some garnet, and have 2–3 modal % of magnetite. Some Idiwhaa samples have higher SiO_2 and in the field contain small, augen-like feldspar and quartz laths[31]. Throughout the mapped area, higher silica Idiwhaa units are found a few metres to the northwest of the more mafic components, although the contact is often obscured. Sample locations are given in refs 20,31.

Modelling of assimilation processes. We employed petrogenetic modelling to evaluate changes in whole-rock and zircon geochemistry through differentiation and assimilation processes that may have influenced the Idiwhaa unit.

First, we used the MELTS software package[32,33] to evaluate the effect of significant fractional crystallization on a primary basaltic magma. No unique fractionation/assimilation scenario gives rise to liquid compositions identical to the Idiwhaa unit samples. However, to model assimilation processes, we used 75% fractional crystallization of an assemblage consisting of 30% plagioclase, 10% olivine and 60% clinopyroxene. This assemblage is comparable to those required to generate modern magmas with similar major-element compositions to the Idiwhaa unit[34–36] using starting magma compositions documented in primitive Icelandic basalts (for example, ref. 36). Significant plagioclase is required to generate the very high FeO, as well as the moderate negative Eu anomalies observed in the Idiwhaa unit. Some portion of olivine is also probably required, as the Ni contents of the Idiwhaa unit are low, even compared to modern icelandite magmas[34,35]. Using the partition coefficients for plagioclase, clinopyroxene and olivine applicable to basaltic liquids[37], along with the mineralogical assemblages described above, we can derive bulk distribution coefficients (D values) for modelling assimilation-fractional crystallization (AFC) processes. Here we have modelled these processes using equations for AFC[38]. Bulk D values for Hf, Yb and La were 0.138805, 0.32346 and 0.10957, respectively.

To model the late-stage assimilation that occurred between Phase I and Phase II zircon crystallization, we used a resulting modelled liquid composition evolved to ~55 wt% SiO_2, lower than the measured Idiwhaa unit, but leaving ample room for potential assimilation of more evolved Archaean TTG-like crust to generate the observed Idiwhaa SiO_2 contents. The modelled liquid composition contained ~26 ppm La, ~8 ppm Yb and ~9 ppm Hf. Using these parameters as one endmember input, and various compositions of TTG-like material as potential assimilants, we performed mixing calculations to derive the elemental and isotopic composition of a potential magma-assimilant mixture. The Archaean Medium-Heavy Rare Earth Element (MHREE) TTG composition was taken from ref. 19 and the average Acasta Gneiss Complex (AGC) TTG was taken from ref. 31 (Archaean MHREE: $La/Yb_N = 26.09$ (ref. 19), $\delta^{18}O = 3.0‰$; 3.6 Gyr AGC TTG: $La/Yb_N = 56.91$ (ref. 31), $\delta^{18}O = 3.0‰$).

The 0.9% decrease in $\delta^{18}O$ between the two igneous zircon phases requires varying amounts of assimilation depending on the assumed assimilant composition. Even in Iceland, a location on the modern Earth that contains a high proportion of low $\delta^{18}O$ rocks, whole rock and corresponding zircon $\delta^{18}O$ values lower than 3.0‰ are uncommon[39–41]. Therefore, we use a $\delta^{18}O$ value of 3.0‰ as a reasonable estimate of the composition of the assimilant, derived from the peak in distribution of Icelandic zircon $\delta^{18}O$ values from ref. 41. Using a starting zircon composition of 5.7‰ and an assimilant value of 3.0‰, ~35% assimilation is required to generate the observed drop in $\delta^{18}O$ values. Using Archaean MHREE TTG as an assimilant[19], any amount of assimilation that is great enough to produce a 0.9‰ drop in the zircon $\delta^{18}O$ values will raise the resulting modelled magma's La_N/Yb_N above those observed in the Idiwhaa unit.

In an attempt to model the derivation of the −2 εHf value documented in Phase I zircon, we used AFC equations[38] with assimilants of variable age and composition. Using the REE and Hf concentrations of MHREE Archaean TTGs[19] we can model how the Hf-isotope composition of this reservoir would change depending on the age of TTG extraction from a chondritic reservoir. For instance, TTG-like Hadean continental crust ($La/Yb_N = 26.09$; ref. 19) with a $^{176}Lu/^{177}Hf$ ratio of 0.0044 that is extracted from a chondritic reservoir at 4,400 Myr will evolve to a $^{176}Hf/^{177}Hf$ ratio of 0.279930 by 4,020 Myr (−8.1 εHf value at 4,020 Myr), while the same composition extracted at 4,200 Myr will evolve to a $^{176}Hf/^{177}Hf$ ratio of 0.280051 (−3.8 εHf) by 4,020 Myr. Mafic crustal compositions were derived from average Hf, Yb and La contents of the Ujaraaluk unit[42] and a $^{176}Lu/^{177}Hf$ of 0.02 (ref. 2). A rock of this composition, extracted from a chondritic reservoir at 4,400 Myr will evolve to a $^{176}Hf/^{177}Hf$ ratio of 0.280042 (−4.1 εHf) by 4,020 Myr.

The AFC modelling equations employed here rely on a key parameter; the mass ratio of cumulates to assimilants (M_c/M_a). This ratio is most significantly dependent on the temperature and solidus of the assimilant country rocks, which effectively determine how much latent heat of crystallization is required to raise the temperature of the assimilant above its solidus. This mass ratio parameter often varies in crustal systems, and has a significant influence over the amount of assimilation possible in a given system. Ref. 43 suggested that small degrees of early crystallization primarily involving olivine could induce early assimilation, suppressing crystallization due to changes in melt composition serving to drive down the M_c/M_a ratio (note that we use the inverse ratio of ref. 43). Geochemically, this low M_c/M_a ratio occurring early in the AFC process allows for large changes in trace element and isotopic composition of the melt with only a small degree of crystallization. We used a moderate M_c/M_a ratio (1.5) in our calculations for Fig. 3b because our modelling is fairly insensitive to this variability in the M_c/M_a ratio. Due to the fact that we are tracking two parameters, La/Yb and εHf, both of which are controlled by elements that are highly incompatible during fractionation of the olivine, clinopyroxene and plagioclase assemblage (La, Yb, Hf) required by the major-element signatures of the Idiwhaa unit, any model using the same input compositions (for example, mafic basalt and TTG) but having variable M_c/M_a will broadly show La/Yb and εHf tracking together. Therefore, changes in the M_c/M_a will mainly change only the amount of assimilation required to produce a given εHf value and La/Yb. This can be seen in Supplementary Fig. 1, where assimilation of the 4,400 Myr mafic composition is modelled using a range of M_c/M_a values. Changes in the M_c/M_a ratio used to model the AFC process do not change the overall pattern of modelled liquid compositions, only the amount of assimilation possible, and therefore the amount of change in liquid composition possible. We note that the amount of assimilation does not drastically influence our model; anything more than a few per cent assimilation of TTG-like crust will drive the La/Yb value of the melt above that observed in the Idiwhaa unit (Fig. 3b). Also note for models involving very low degrees of assimilation (that is, high remaining liquid proportions; Supplementary Fig. 1) that a small increase in La_N/Yb_N will occur throughout the rest of the differentiation sequence, on the order of ~1 unit of La_N/Yb_N. Therefore, models where assimilation creates a lower La_N/Yb_N at −2 εHf than that seen in the Idiwhaa unit, such as that created by AFC modelling of 4,400 Myr mafic crust with an M_c/M_a ratio of 1.1, are still petrologically acceptable.

Sm–Nd isotopic analysis. Rock powders were spiked with a known amount of mixed ^{150}Nd–^{149}Sm tracer solution—this tracer was calibrated directly against the Caltech mixed Sm/Nd standard[44]. Dissolution in mixed 24N HF + 16N HNO_3 at 160 °C for five days preceded chloride conversion with HCl, and Nd and Sm separation by conventional cation and di(2-ethyl hexyl phosphate)-based (Eichron LN Resin) chromatography.

Chemical processing blanks were <200 pg for either Sm or Nd, and were insignificant relative to the amount of Sm or Nd analysed for any rock sample. Further details can be found in refs 45,46. The isotopic composition of Nd was determined in static mode by multi-collector inductively coupled plasma mass spectrometry (MC-ICP-MS)[47]. All isotope ratios were normalized for variable mass fractionation to a value of $^{146}Nd/^{144}Nd = 0.7219$ using the exponential fractionation law. The $^{143}Nd/^{144}Nd$ ratio of samples were presented relative to a value of 0.511850 for the La Jolla Nd isotopic standard, monitored using an in-house Alfa Nd isotope standard for each analytical session. Sm isotopic abundances were measured in static mode by MC-ICP-MS, and were normalized for variable mass fractionation to a value of 1.17537 for $^{152}Sm/^{154}Sm$, also using the exponential law. Using the same isotopic analysis and normalization procedures as above, we analyzed the Nd isotope standard 'Shin Etsu: JNdi-1' as an unknown[48], which has a $^{143}Nd/^{144}Nd$ value of 0.512107 relative to a LaJolla $^{143}Nd/^{144}Nd$ value of 0.511850.

The value of $^{143}Nd/^{144}Nd$ determined for the JNdi-1 standard conducted during the analysis of the nine samples reported here was 0.512097 ± 8 (2 s.e.); the long-term average value was 0.512098 ± 10 (1 s.d., $n = 88$, past eight years). Using the mixed ^{150}Nd–^{149}Sm tracer, the measured $^{147}Sm/^{144}Nd$ ratios for the international rock standard BCR-1 range from 0.1380 to 0.1382, suggesting reproducibility for $^{147}Sm/^{144}Nd$ of ± 0.1% for real rock powders.

LASS Hf methods. Concurrent Hf and U–Pb isotope measurements using laser-ablation split-stream (LASS) protocols broadly followed the methods of ref. 49. Measurements were made in the Arctic Resources Laboratory at the University of Alberta using a Resonetics Excimer 193 nm laser operating with an energy fluence of 5 J cm^{-2} at 10 Hz with a 33 μm diameter spot size. U–Pb isotope measurements were made on a Thermo Element-XR mass spectrometer using a single secondary electron multiplier (SEM) detector in peak hopping mode, while Hf isotope measurements were made on a Thermo Neptune Plus using multiple Faraday detectors with 10^{11} Ω amplifiers operating in static mode. Analysis time was typically 90 s, consisting of 20 s of background followed by 40 s of ablation and 30 s of washout. Both Hf and U–Pb data were processed offline using Iolite v3 software, where integrations were chosen very carefully and trimmed to remove portions with highly variable U–Pb or Hf-isotope compositions

Both Hf and U–Pb analytical biases were calibrated using Plešovice zircon as a primary reference material[50]. Due to the large corrections necessary for the isobaric interference of ^{176}Yb on the ^{176}Hf signal, combined with relatively low Yb contents in Plešovice zircon (average $^{176}Yb/^{177}Hf = 0.006$), it is absolutely essential to evaluate other reference materials with higher concentrations of Yb[51] that more closely approximate the samples analysed here. For this we monitored the Yb-interference correction by analysis of FC1 and R33 (natural zircons) with Yb

contents and Yb/Hf in the range of most natural zircons[49], and Yb-doped zircons (MUN1 and MUN4[51]; synthetic) were also evaluated, with MUN4 containing a much greater concentration of Yb and hence much higher Yb/Hf than the TC3 zircon unknowns analysed here. The measured $^{176}Yb/^{173}Yb$ ratio was iteratively calibrated to optimize the Yb-interference correction, monitored by five zircon reference materials with variable Yb contents (Plešovice, FC1, R33, MUN1, MUN4) in the same manner as that of ref. 50.

Due to the complexity of TC3 zircons, the quality of each analysis was evaluated by monitoring both U–Pb and Pb–Pb ratios throughout the length of the analysis. Consistent U–Pb and Pb–Pb ratios throughout each run indicated that the analysis volume probably consisted of one growth phase, and the Hf-isotope composition of the integration represents that of a particular domain. The relative reliability of each analysis was evaluated using the length of selected integration relative to the total ablation duration. Analyses where a substantial (>70%) portion of the analysis was retained were deemed highly reliable. Analyses where ~30–70% of the run was consistent in both U–Pb and Hf composition were deemed moderately reliable and retained, whereas analyses with <30% of the ablation returning consistent data were deemed unreliable and cut from further evaluation (Supplementary Fig. 2).

All initial εHf values and fully propagated uncertainties were calculated using the equations from ref. 52 and calculated at 4,020 Myr, the igneous crystallization age of the unit (Fig. 1). This method is valid for several reasons. First, although zircon material with igneous zoning characteristics does contain small degrees of Pb loss (Supplementary Figs 5 and 6 of ref. 20), this Pb loss probably does not affect the Hf-isotope composition of the zircon. Hf is incorporated into the zircon crystal structure during crystallization, and is lattice bound[53], whereas Pb is created by decay of U. Heating or fluid interactions may mobilize Pb from the zircon structure, whereas Hf should remain unaffected[54,55]. Additionally, LASS U–Pb analyses have substantially lower precision than other methods reported here (ID-TIMS) and previously (SIMS[20]). Therefore, we deem both the ID-TIMS and SIMS U–Pb age more accurate and reliable than the U–Pb ages generated during LASS, which were collected to monitor the heterogeneity of the zircon volume analysed during laser-ablation Hf analyses. Results for TC3 zircon that had fully propagated uncertainties in εHf exceeding ±4 epsilon units were filtered out of all future calculations ($n=4$).

CA-ID-TIMS U–Pb and solution Hf. An aggressive chemical abrasion procedure was applied to zircons extracted from the TC3 sample. To test the efficacy of the chemical abrasion technique on these ancient zircons, we first applied a simple chemical abrasion procedure[56] comprising 48 h annealing at 1,000 °C followed by 19 h of chemical abrasion in 24N HF and trace HNO_3 at 190 °C. These grains were analysed only for their U–Pb systematics following the methods described below, with no *in situ* information collected from these samples (grey symbols in Fig. 1).

A second batch of TC3 zircons was first characterized using cathodoluminescence imaging and electron microprobe (EPMA) analyses of Y contents before dissolution. This process entailed annealing at 1,000 °C for 48 h, followed by 24 h of chemical abrasion at 190 °C in 24N HF with trace HNO_3. Fragments of grains that survived the chemical abrasion procedure were mounted in epoxy and imaged using both cathodoluminescence and backscatter electron to identify fragments that were dominated by single growth zones. Previous SIMS trace-element measurements of Phase I and II zircon material identified a dramatic difference in Y contents (Phase I = 2,000–3,000 ppm Y; Phase II = 700–800 ppm Y; ref. 20), quantifiable by EPMA. We analysed the mounted and imaged grains for Y contents by EPMA (University of Alberta) to assist in identification of the two igneous growth zones. Major elements (Zr, Si) as well as a suite of trace elements (Ca, Y, P, Yb) were analysed on the JEOL 8900R EPMA using a 15 kV accelerating voltage and a 50 nA current. Grains with simple zoning patterns and consistent trace-element concentrations were plucked out of the mount and subjected to a further five hours of chemical abrasion in 24N HF and trace HNO_3 at 190 °C; these fragments were then ready for dissolution following the procedures of refs 57,58.

Before dissolution, all of the grain fragments were cleaned and spiked with ~5 ml of EARTHTIME ^{202}Pb–^{205}Pb–^{233}U–^{235}U spike, then placed in Parr bombs at 210 °C with ~70 µl of HF and trace HNO_3 for 48 h. After dissolution, U and Pb were extracted using HCl-based anion exchange column chemistry[59]. The Zr and Hf washes were collected for Hf isotope analysis. Once separated, the U–Pb fraction was loaded onto outgassed Re filaments with a Si-Gel emitter[60] and trace H_3PO_4. U and Pb isotopic measurements were conducted on a Thermo TRITON thermal ionization mass spectrometer, where Pb and U were measured in dynamic mode on a MassCom secondary electron multiplier. Pb fractionation was controlled using a $^{202}Pb/^{205}Pb$ of 0.99924 ± 0.00027 (1σ absolute[61]). U was measured as an oxide and the interferences from $^{233}U^{18}O^{16}O$ on $^{235}U^{16}O_2$ were corrected using an $^{18}O/^{16}O$ of 0.00205. U/Pb ratios were calculated relative to a $^{235}U/^{205}Pb$ of 100.23 ± 0.023% (1σ abs) and the $^{238}U/^{235}U$ of the samples was assumed to be 137.818 ± 0.045 (2σ; ref. 62). All data reduction was performed using Tripoli and Redux software[63], using the algorithms of ref. 64.

Solution Hf isotope analyses were performed at the University of Geneva using a Thermo Neptune plus MC-ICP-MS with nickel cones (Thermo 'X series') under dry plasma conditions using a Cetac 'Aridus 2' desolvation unit following the procedure of ref. 65. Hf fractions collected during U–Pb column chemistry were re-dissolved in 2% HNO_3 and trace HF to minimize memory effects. A Plešovice zircon[50] solution at a Hf concentration of ~10 ppb was doped with variable amounts of Yb (ICP-MS standard solution, Merck KGaA), so that Yb concentrations range from $0.001 < {}^{173}Yb/^{177}Hf < 0.5$; these solution were used to optimize the ^{176}Yb-interference correction[65] and to determine a normalization factor from the reference value of ref. 50. Several grains of Temora-2[66] were also measured as secondary standards and normalized following the factor determined by the doped Plešovice.

Hf isotope measurements were employed following the short acquisition time measurements and sample-standard bracketing procedures outline in ref. 65. The βYb and βHf mass bias coefficients were calculated using an exponential law[67] from the measured $^{172}Yb/^{173}Yb$ and $^{179}Hf/^{177}Hf$, respectively, and using natural abundances reference values: $^{172}Yb/^{173}Yb = 1.3534$ and $^{179}Hf/^{177}Hf = 0.7325$ (ref. 68). Mass bias correction on Lu was calculated using βYb (ref. 69) and the isobaric interference of ^{176}Lu was removed using the natural abundances of ^{175}Lu (0.97416) and ^{176}Lu (0.02584). The isobaric interference of ^{176}Yb was evaluated from Yb-doped Plešovice solutions by calculating $^{176}Yb/^{173}Yb$ using βYb and a reference value that is empirically determined for each run by minimizing the drift in corrected $^{176}Hf/^{177}Hf$ ratios for increasing $^{173}Yb/^{177}Yb$ (ref. 65), as shown by ref. 49. The optimized value of $^{176}Yb/^{173}Yb$ was 0.787000, which is within 0.015% of the natural Yb isotope composition ($^{176}Yb/^{173}Yb = 0.786956$; ref. 70). Correction for ^{176}Hf in-growth due to ^{176}Lu decay has been calculated using $^{176}Lu = 1.87 \times 10^{-11}$ year^{-1} and the age determined by the ID-TIMS U–Pb dating. During the measurement session, the $^{176}Hf/^{177}Hf$ ratio for Plešovice was 0.282481 ± 40 (2 s.d., $n=11$) and the normalized Temora-2 $^{176}Hf/^{177}Hf$ ratio was 0.282666 ± 62 (2 s.d., $n=7$).

Data availability. All data used here are reported in the Supplementary Tables, and additional information regarding sample locations and photos can be made available from the corresponding author upon request.

References

31. Reimink, J. R., Chacko, T., Stern, R. A. & Heaman, L. M. The birth of a cratonic nucleus: lithogeochemical evolution of the 4.02–2.94 Ga Acasta Gneiss Complex. *Precambr. Res.* **281,** 453–472 (2016).
32. Gualda, G. A. R., Ghiorso, M. S., Lemons, R. V. & Carley, T. L. Rhyolite-MELTS: a modified calibration of MELTS optimized for silica-rich, fluid-bearing magmatic systems. *J. Petrol.* **53,** 875–890 (2012).
33. Ghiorso, M. S. & Gualda, G. A. R. An H_2O–CO_2 mixed fluid saturation model compatible with rhyolite-MELTS. *Contrib. Mineral Petrol.* **169,** 53–30 (2015).
34. Wood, D. A. Major and trace element variations in the tertiary lavas of Eastern Iceland and their significance with respect to the Iceland geochemical anomaly. *J. Petrol.* **19,** 393–436 (1978).
35. Jónasson, K. Magmatic evolution of the Heiðarsporður ridge, NE-Iceland. *J. Volcanol. Geotherm. Res.* **147,** 109–124 (2005).
36. Mancini, A., Mattsson, H. B. & Bachmann, O. Origin of the compositional diversity in the basalt-to-dacite series erupted along the Heiðarsporður ridge, NE Iceland. *J. Volcanol. Geotherm. Res.* **301,** 116–127 (2015).
37. Rollinson, H. R. *Using Geochemical Data* (Pearson Education Limited, 1993).
38. Taylor, H. P. & Sheppard, S. M. F. Igneous rocks I: processes of isotopic fractionation and isotope systematics. *Rev. Mineral. Geochem.* **16,** 227–271 (1986).
39. Muehlenbachs, K., Anderson, A. T. & Sigvaldason, G. E. Low-O^{18} basalts from Iceland. *Geochim. Cosmochim. Acta* **38,** 577–588 (1974).
40. Eiler, J. M. Oxygen isotope variations of basaltic lavas and upper mantle rocks. *Rev. Mineral. Geochem.* **43,** 319–364 (2001).
41. Carley, T. L. *et al*. Iceland is not a magmatic analog for the Hadean: evidence from the zircon record. *Earth Planet. Sci. Lett.* **405,** 85–97 (2014).
42. O'Neil, J., Boyet, M., Carlson, R. W. & Paquette, J.-L. Half a billion years of reworking of Hadean mafic crust to produce the Nuvvuagittuq Eoarchean felsic crust. *Earth Planet. Sci. Lett.* **379,** 13–25 (2013).
43. Reiners, P. W., Nelson, B. K. & Ghiorso, M. S. Assimilation of felsic crust by basaltic magma: thermal limits and extents of crustal contamination of mantle-derived magmas. *Geology* **23,** 563–566 (1995).
44. Wasserburg, G. J., Jacousen, S. B., DePaolo, D. J., McCulloch, M. T. & Wen, T. Precise determination of ratios, Sm and Nd isotopic abundances in standard solutions. *Geochim. Cosmochim. Acta* **45,** 2311–2323 (1981).
45. Creaser, R. A., Erdmer, P., Stevens, R. A. & Grant, S. L. Tectonic affinity of Nisutlin and Anvil assemblage strata from the Teslin tectonic zone, northern Canadian Cordillera: constraints from neodymium isotope and geochemical evidence. *Tectonics* **16,** 107–121 (1997).
46. Unterschutz, J. L., Creaser, R. A., Erdmer, P., Thompson, R. I. & Daughtry, K. L. North American margin origin of Quesnel terrane strata in the southern Canadian Cordillera: inferences from geochemical and Nd isotopic characteristics of Triassic metasedimentary rocks. *Geol. Soc. Am. Bull.* **114,** 462–475 (2002).

47. Schmidberger, S. S., Simonetti, A., Heaman, L. M., Creaser, R. A. & Whiteford, S. Lu–Hf, in-situ Sr and Pb isotope and trace element systematics for mantle eclogites from the Diavik diamond mine: evidence for Paleoproterozoic subduction beneath the Slave craton, Canada. *Earth Planet. Sci. Lett.* **254,** 55–68 (2007).
48. Tanaka, T. *et al*. JNdi-1: a neodymium isotopic reference in consistency with LaJolla neodymium. *Chem. Geol.* **168,** 279–281 (2000).
49. Fisher, C. M., Vervoort, J. D. & DuFrane, S. A. Accurate Hf isotope determinations of complex zircons using the 'laser ablation split stream' method. *Geochem. Geophys. Geosyst.* **15,** 121–139 (2014).
50. Sláma, J. *et al*. Plešovice zircon—a new natural reference material for U–Pb and Hf isotopic microanalysis. *Chem. Geol.* **249,** 1–35 (2008).
51. Fisher, C. M. *et al*. Synthetic zircon doped with hafnium and rare earth elements: a reference material for *in situ* hafnium isotope analysis. *Chem. Geol.* **286,** 32–47 (2011).
52. Ickert, R. B. Algorithms for estimating uncertainties in initial radiogenic isotope ratios and model ages. *Chem. Geol.* **340,** 1–43 (2013).
53. Hoskin, P. W. O. The composition of zircon and igneous and metamorphic petrogenesis. *Rev. Mineral. Geochem.* **53,** 27–62 (2003).
54. Lenting, C. *et al*. The behavior of the Hf isotope system in radiation-damaged zircon during experimental hydrothermal alteration. *Am. Mineral.* **95,** 1343–1348 (2010).
55. Amelin, Y., Kamo, S. L. & Lee, D.-C. Evolution of early crust in chondritic or non-chondritic Earth inferred from U–Pb and Lu–Hf data for chemically abraded zircon from the Itsaq Gneiss Complex, West Greenland. *Can. J. Earth Sci.* **48,** 141–160 (2011).
56. Mattinson, J. M. Zircon U–Pb chemical abrasion ('CA-TIMS') method: combined annealing and multi-step partial dissolution analysis for improved precision and accuracy of zircon ages. *Chem. Geol.* **220,** 47–66 (2005).
57. Wotzlaw, J. F. *et al*. Tracking the evolution of large-volume silicic magma reservoirs from assembly to supereruption. *Geology* **41,** 867–870 (2013).
58. Davies, J. H. F. L., Wotzlaw, J.-F., Wolfe, A. P., Heaman, L. M. & Arbour, V. Assessing the age of the Late Cretaceous Danek Bonebed with U–Pb geochronology. *Can. J. Earth Sci.* **51,** 982–986 (2014).
59. Krogh, T. E. A low-contamination method for hydrothermal decomposition of zircon and extraction of U and Pb for isotopic age determinations. *Geochim. Cosmochim. Acta* **37,** 485–494 (1973).
60. Gerstenberger, H. & Haase, G. A highly effective emitter substance for mass spectrometric Pb isotope ratio determinations. *Chem. Geol.* **136,** 309–312 (1997).
61. Condon, D. J., Schoene, B., McLean, N. M., Bowring, S. A. & Parrish, R. R. Metrology and traceability of U–Pb isotope dilution geochronology (EARTHTIME Tracer Calibration Part I). *Geochim. Cosmochim. Acta* **164,** 464–480 (2015).
62. Hiess, J., Condon, D. J., McLean, N. & Noble, S. R. 238U/235U systematics in terrestrial uranium-bearing minerals. *Science* **335,** 1610–1614 (2012).
63. Bowring, J. F., McLean, N. M. & Bowring, S. A. Engineering cyber infrastructure for U–Pb geochronology: Tripoli and U–Pb_Redux. *Geochem. Geophys. Geosyst.* **12,** Q0AA19 (2011).
64. McLean, N. M., Bowring, J. F. & Bowring, S. A. An algorithm for U–Pb isotope dilution data reduction and uncertainty propagation. *Geochem. Geophys. Geosyst.* **12,** Q0AA18 (2011).
65. D'Abzac, F.-X., Davies, J. H. F. L., Wotzlaw, J.-F. & Schaltegger, U. Hf isotope analysis of small zircon and baddeleyite grains by conventional multi collector-inductively coupled plasma-mass spectrometry. *Chem. Geol.* **433,** 12–23 (2016).
66. Wu, F.-Y., Yang, Y.-H., Xie, L.-W., Yang, J.-H. & Xu, P. Hf isotopic compositions of the standard zircons and baddeleyites used in U–Pb geochronology. *Chem. Geol.* **234,** 105–126 (2006).
67. Albarede, F. *et al*. Precise and accurate isotopic measurements using multiple-collector ICPMS. *Geochim. Cosmochim. Acta* **68,** 2725–2744 (2004).
68. Blichert-Toft, J. & Albarède, F. The Lu–Hf isotope geochemistry of chondrites and the evolution of the mantle-crust system. *Earth Planet. Sci. Lett.* **148,** 243–258 (1997).
69. Yuan, H. *et al*. Simultaneous determinations of U–Pb age, Hf isotopes and trace element compositions of zircon by excimer laser-ablation quadrupole and multiple-collector ICP-MS. *Chem. Geol.* **247,** 100–118 (2008).
70. Thirlwall, M. F. & Anczkiewicz, R. Multidynamic isotope ratio analysis using MC–ICP–MS and the causes of secular drift in Hf, Nd and Pb isotope ratios. *Int. J. Mass Spectrom.* **235,** 59–81 (2004).